Progress In Electromagnetics Research, PIER 75, 163–170, 2007

GENERATION OF HIGH REPETITION RATE PICOSECOND PULSE TRAIN BASED ON ULTRA-SMALL SILICON WAVEGUIDE

J.-W. Wu and F.-G. Luo

School of Optoelectronic Science and Engineering
Huazhong University of Science and Technology
Wuhan 430074, China

Abstract—A designed model based on the ultra-small silicon waveguide(WG) is demonstrated to generate high repetition rate picosecond pulse train. Research result shows that 50 GHz repetition rate pulse can be obtained inside a 2-mm-long ultra-small silicon WG using signal wave at 1550 nm with a cw power of 0.2 mW and different delay modulation Gaussian pulses at 1670 nm with peak of 0.6 mW before the WG. the signal pulse train obtained has duration time as short as around 6 ps full width of half maximum(FWHM) and extinction ratio as large as up to 30 dB. Additionally, each pulse of signal pulse train obtained holds equal intensity and close Gaussian waveform.

1. INTRODUCTION

Silicon photonics has recently attracted a great deal of attention since it is a promising platform for low cost solutions to photonic integrated circuits and optoelectronic devices [1, 2]. However, light emission and amplification are very difficult for silicon WG owing to its indirect bandgap. One found that the Raman effect is roughly 10^4 times stronger in silicon than for silica fiber, so the stimulated Raman scattering could be used for overcoming its limitation and making the silicon an active material. In fact, it isn't still easy for observing the Raman amplification in bold silicon because of the free-carrier absorption (FCA) that arises from two-photon absorption (TPA). The strength of FCA depends upon how much the carriers accumulate in the WG core before recombining. This is quantified by effective charg-carrier lifetime, which is lower when carriers quickly recombine or diffuse out of the silicon core. So far, some technologies are developed

to reduce the carrier lifetime and all kinds of applications are achieved by using silicon WG, such as raman laser, raman amplification, all-optical switching, slow light, and wavelength conversion, etc. [3–9]. In this paper, for the first time we believe, in order to generate the high repetition rate pulse train, which is a critical technique in current and future optical networks, we have designed a theoretical model utilizing the ultra-small silicon WG structure. The model designed and pulse train obtained have many advantages as compared to previous works, such as our pulse source is integrated, each pulse of output signal pulse train has equal intensity, symmetrical waveform, and larger extinction ratio.

2. MODEL & THEORY

Figure 1 is our designed theoretical model showing the principle to generate the high repetition rate picosecond pulse train in ultra-small silicon WG. A Gaussian modulation pulse is divided into N equivalent pulses by $1 \times N$ coupler, then each pulse divided will experience different route with equal delay time ΔT for adjacent two routes. The delay modulation pulses and cw signal wave are combined with a wavelength division multiplexer (WDM) into a single-mode optical fiber, whose output is coupled into the silicon WG, and will produce nonlinear interaction in WG. Then the output beam of the WG goes through the optical filter, which is used to separate the modulation and signal beams, and the signal beam only passes through the filter.

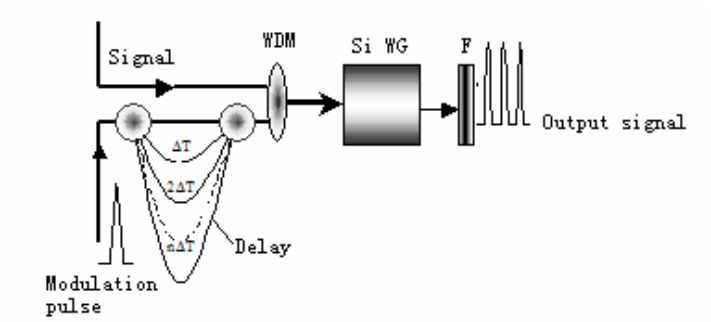

Figure 1. Designed model based on silicon WG for generating the high repetition rate picosecond pulse train. Signal: 1550 nm cw wave, Modulation pulse: 1670 nm Gaussian pulse.

Since the Raman response time is ~ 3 ps in ultra-small silicon WG, for pulse much longer than 3 ps, the raman response can be treated as being instantaneous. The nonlinear propagation equation is similar to

the standard equation used to describe pulse dynamic in optical fiber [10, 11], but will include additional terms describing the effects of TPA, and FCA. So the signal and modulation beam will satisfy the following coupled propagation equations [12]:

$$\begin{aligned}
&\frac{\partial A_s}{\partial Z}+i\frac{\beta_{2s}}{2}\frac{\partial^2 A_s}{\partial T^2}\\
&=-\frac{c\beta_{1s}k_s}{2n_s}\left(\alpha_{in}+\alpha_{FC}^s\right)A_s+i\frac{\omega_s\beta_{1s}k_s}{n_s}\delta n_{FC}^s A_s\\
&\quad+i\frac{3\omega_s\beta_{1s}^2}{\varepsilon_0 S}\Big(\Gamma_s\left|A_s\right|^2+2\Gamma_{ms}\left|A_m\right|^2\Big)A_s+i\frac{6\omega_s\beta_{1s}^2}{\varepsilon_0 S}\Gamma_R^s\left(-\omega_R\right)\left|A_m\right|^2A_s \quad (1)\\
&\frac{\partial A_m}{\partial Z}-d\frac{\partial A_m}{\partial T}+i\frac{\beta_{2m}}{2}\frac{\partial^2 A_m}{\partial T^2}\\
&=-\frac{c\beta_{1m}k_m}{2n_m}\left(\alpha_{in}+\alpha_{FC}^m\right)A_m+i\frac{\omega_m\beta_{1m}k_m}{n_m}\delta n_{FC}^m A_m\\
&\quad+i\frac{3\omega_m\beta_{1m}^2}{\varepsilon_0 S}\Big(\Gamma_m\left|A_m\right|^2+2\Gamma_{sm}\left|A_s\right|^2\Big)A_m+i\frac{6\omega_c\beta_{1c}^2}{\varepsilon_0 S}\Gamma_R^s(\omega_R)\left|A_s\right|^2A_m \quad (2)
\end{aligned}$$

where subscript s and m denote the signal and modulation beam, A, β_2 and ω are the slowly varying amplitude, group velocity dispersion parameter and angle frequency, respectively, Z is the propagation distance, T is the time in the moving frame of the signal wave, d is the group-velocity mismatch parameter between two beams, c is the light velocity in vacuum, α_{in} is the linear loss, $n(=\varepsilon+\frac{A}{\lambda^2}+\frac{B\lambda_1^2}{\lambda^2-\lambda_1^2}$, with $\varepsilon=11.6858$, $A=939816\,\mathrm{nm}^2$, $B=0.00810461$, $\lambda_1=1107.1\,\mathrm{nm}$) is the refractive index of unperturbed, S is the transverse area of the WG, k is the WG constant, ε_0 is permittivity of free space, Γ is the susceptibility, α_{FC} and δn_{FC} are the change in the refractive index and FCA coefficient, respectively, and based on the classical Drude model of the free carriers, which can be described by [13]

$$\delta n_{FC} = -\frac{e^2\lambda_{s(m)}^2}{8\pi^2c^2\varepsilon_0 n_{s(m)}}\left[\frac{N_e}{0.26m_0}+\frac{N_h}{0.39m_0}\right] \quad (3)$$

$$\alpha_{FC} = \frac{e^3\lambda_{s(m)}^2}{4\pi^2c^3\varepsilon_0 n_s(m)}\left[\frac{N_e}{\mu_e(0.26m_0)^2}+\frac{N_h}{\mu_h(0.39m_0)^2}\right] \quad (4)$$

where e is the charge of the electron, λ is the wavelength, N_e and N_h are the induced variation of the electrons and holes density, respectively, μ_e and μ_h are the electron and hole mobility, m_0 is the mass of the electron.

For describing the dynamics of optical pulses interaction in silicon WG, the variety of free carriers density must take into account in different time and locality. Assuming equal free electrons and holes in WG, the rate equation of the electron and hole pairs density can be written as [12]:

$$\frac{dN}{dT} = -\frac{N}{\tau_c} + \frac{6}{\varepsilon_0 \hbar S^2}\left(\frac{\beta_{1s}^2 \Gamma_s''}{2}|A_s|^4 + \frac{\beta_{1m}^2 \Gamma_m''}{2}|A_m|^4 + 2\frac{\omega_s \beta_{1s}^2 \Gamma_{ms}'' + \omega_m \beta_{1m}^2 \Gamma_{sm}''}{\omega_s + \omega_m}|A_s|^2 |A_m|^2\right) \quad (5)$$

where τ_c is the effective carriers lifetime, β_1 is the first order dispersion parameter. The equations (1)–(5) can be numerically solved by the well-known finite-difference time-domain (FDTD) method [14–16].

3. RESULTS & ANALYSIS

For the typical ultra-small silicon WG (0.45 um, 0.22 um), when the signal and modulation wavelengths are equal to 1550 nm and 1670 nm, respectively, the corresponding system parameters of the silicon WG are $\beta_{1s} = 1.37 \times 10^4$ ps/m, $\beta_{1m} = 1.38 \times 10^4$ ps/m, $\beta_{2s} = -1.20\,\mathrm{ps}^2/\mathrm{m}$, $\beta_{2m} = 0.60\,\mathrm{ps}^2/\mathrm{m}$, $m_0 = 9.10939 \times 10^{-31}$ Kg, $\alpha_{in} = 3.5$ dB/cm, $\varepsilon_0 = 8.854 \times 10^{-12}\,\mathrm{C}^2/\mathrm{Jm}$, $\tau_c = 1$ ns, $k_s = 0.907$, $k_m = 0.871$, $\Gamma_R^s(-\omega_R) = i2.1 \times 10^{-18}\,\mathrm{m}^2/\mathrm{V}^2$, $\Gamma_R^m(\omega_R) = -i1.8 \times 10^{-18}\,\mathrm{m}^2/\mathrm{V}^2$, $\Gamma_s = 7.76 \times 10^{-20} + i4.97 \times 10^{-21}\,\mathrm{m}^2/\mathrm{V}^2$, $\Gamma_{sm}'' = 5.09 \times 10^{-21}\,\mathrm{m}^2/\mathrm{V}^2$, $\Gamma_{ms}'' = 4.35 \times 10^{-21}\,\mathrm{m}^2/\mathrm{V}^2$, $\Gamma_m = 6.95 \times 10^{-20} + i4.45 \times 10^{-21}\,\mathrm{m}^2/\mathrm{V}^2$, $\Gamma_{sm} = 6.79 \times 10^{-20} + i4.35 \times 10^{-21}\,\mathrm{m}^2/\mathrm{V}^2$, $\Gamma_{ms} = 7.94 \times 10^{-20} + i5.09 \times 10^{-21}\,\mathrm{m}^2/\mathrm{V}^2$, $\Gamma_s'' = 4.97 \times 10^{-21}\,\mathrm{m}^2/\mathrm{V}^2$, $\Gamma_m'' = 4.45 \times 10^{-21}\,\mathrm{m}^2/\mathrm{V}^2$.

Figure 2 shows that the normal output waveform of obtained high repetition rate pulse train after 2-mm-long silicon WG and the input profile of delay modulation pulse before silicon WG. In our calculation, a cw signal wave with 0.20 mW power and a Gaussian modulation pulse with 0.6 mW peak and 8.33 ps FWHM, $\Delta T = 20$ ps, the extinction ratio of profile of modulation pulse is 9.45 dB. From the figure, it is seen that picosecond pulse train obtained has 50 GHz high repetition rate and equal intensity for each pulse. moreover, there is invert phase difference between signal and modulation pulse, and the signal pulse has as short as around 6 ps FWHM and as large as 32.60 dB extinction ratio by calculation. These can be explained that the cw signal and modulation pulse are co-propagating, the energy of signal wave will convert to the modulation pulse at the Stokes frequency due to strong stimulated Raman scatting in silicon WG. The efficiency of energy

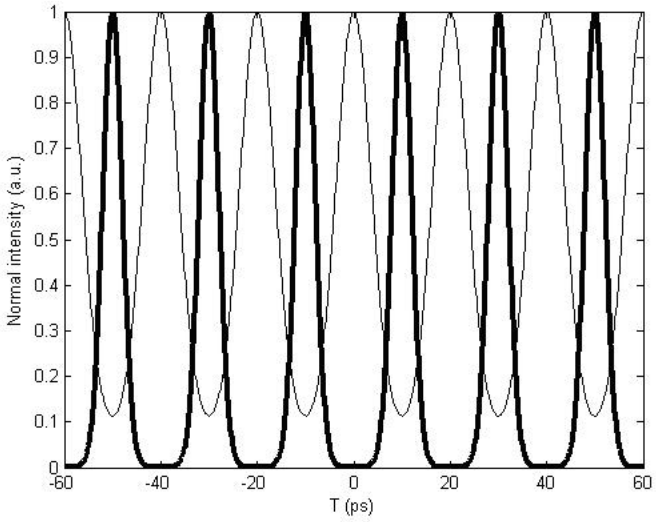

Figure 2. Output waveform of obtained signal pulse train (thick line) and input profile of delay modulation pulse (thin line).

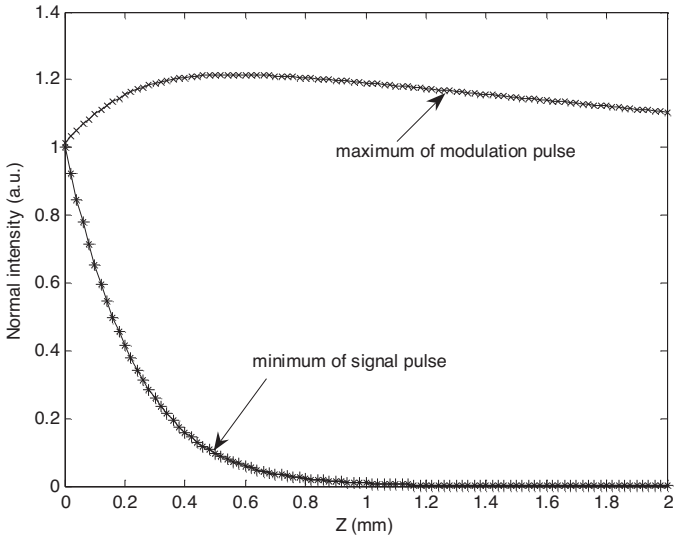

Figure 3. Variety curves of signal pulse minimum and modulation pulse maximum against the length of silicon WG.

conversion is proportional to the energy of modulation pulse. Delay modulation pulse will modulate periodically the cw signal wave, then high quality signal pulse train, whose period is decided by the delay time ΔT, can be obtained in the output port of WG. The phase of signal pulse train is invert comparative to modulation, namely, minimum of signal pulse is opposite to maximum of modulation pulse. In Figure 3, we plot the variety curves of minimum of signal pulse and maximum of modulation pulse against the transmission distance in silicon WG. from the figure, we can see that the minimum of signal pulse will be decreased gradually with the distance increased, and the energy of signal wave converted to the modulation wave. As a result, energy of modulation pulse will be increased gradually, but the peak power will be decreased again after a certain transmission distance owing to the linear loss, FCA and group velocity dispersion. However the effects of FCA and GVD are slightly to the 2-mm-long silicon WG and low intensity pulse. The linear loss will play a significant role for the decrease of modulation pulse peak power.

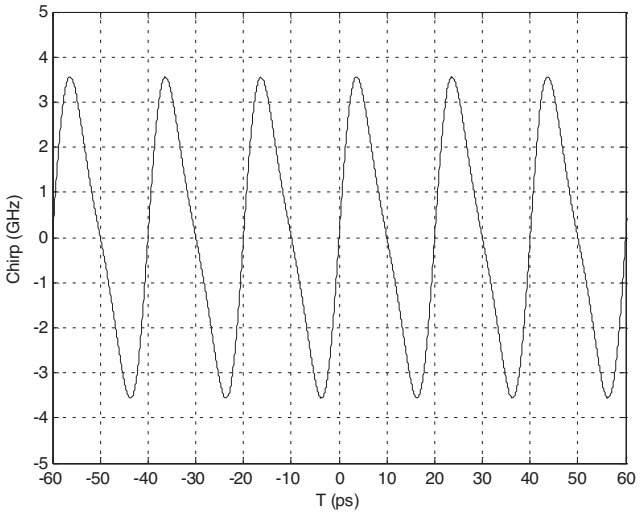

Figure 4. The chirp curve of output signal pulse train.

Figure 4 shows the chirp curve of signal pulse train at the output port. From the figure, it is seen that it has equal chirp value at the leading edge and tailing edge of each output pulse. Negative chirp (decreased linearly) is induced at the center part of pulse due to the the cross-phase modulation effect between signal and modulation pulse. What's more, the output waveform of signal pulse is very close to the Gaussian pulse, which is shown in Figure 5.

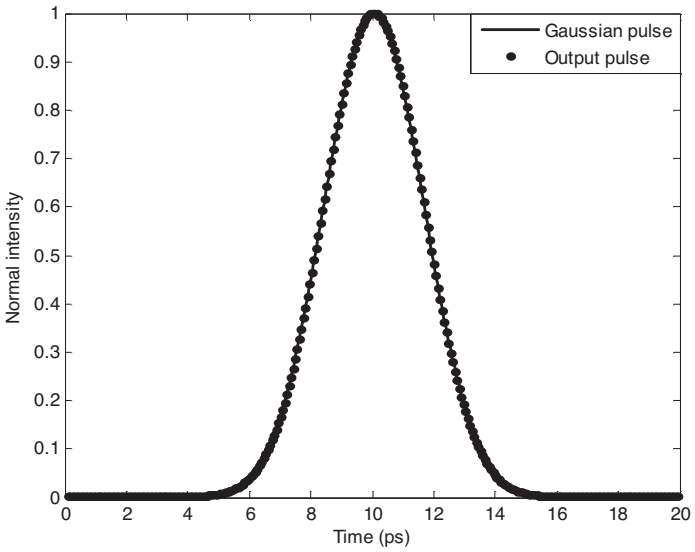

Figure 5. The waveforms of output signal pulse (dotted line) and Gaussian pulse (continue line) with the same peak power and full width half maximum as that of signal pulse.

4. CONCLUSION

We for the first time designed the model of generation of high repetition rate picosecond pulse train. The property of signal pulse train obtained is researched by numerical simulation. 50 GHz repetition rate picosecond pulse train, which has short width, high extinction ratio, uniform waveform and negative chirp at the pulse's center part, can be obtained by using our designed model.

REFERENCES

1. Pavesi, L. and D. J. Lockwood, *Silicon Photonics*, Springer-Verlag, New York, 2004.
2. Reed, G. T. and A. P. Knights, *Silicon Photonics: An Introduction*, John Wiley, West Sussex, 2004.
3. Rong, H., A. Liu, R. Jones, O. Cohen, D. Hak, R. Nicolaescu, A. Fang, and M. Paniccia, "An all-silicon Raman laser," *Nature*, Vol. 433, No. 17, 292–294, 2005.

4. Rong, H., R. Jones, Liu A., O. Cohen, D. Hak, A. Fang, and M. Paniccia, "A continuous-wave Raman silicon laser," *Nature*, Vol. 433, No. 20, 725–728, 2005.
5. Liang, T. and H. Tsang, "Efficient Raman amplification in silicon-on-insulator waveguide," *Appl. Phys. Lett.*, Vol. 85, No. 16, 3343–3345, 2004.
6. Liu, A., H. Rong, R. Jones, O. Cohen, D. Hak, and M. Paniccia, "Optical amplification and lasing by stimulated Raman scattering in silicon waveguides," *J. Lightwave Technol.*, Vol. 24, No. 3, 1440–1455, 2006.
7. Almeida, V., R. Barrios, R. Panepucci, and M. Lipson, "All-optical control of light on a silicon chip," *Nature*, Vol. 431, No. 28, 1081–1084, 2004.
8. Blair, S. and K. Zheng, "Intensity-tunable group delay using stimulated Raman scattering in silicon slow-light waveguides," *Opt. Express*, Vol. 14, No. 3, 1064–1069, 2006.
9. Rong, H., Y. Kuo, A. Liu, M. Paniccia, and O. Cohen, "High efficiency wavelength conversion of 10 Gb/s data in silicon waveguides," *Opt. Express*, Vol. 14, No. 3, 1182–1188, 2006.
10. Shweanshumala, A. Biswas, and S. Konar, "Dynamically stable super Gaussian solitons in semiconductor doped glass fibers," *J. of Electromagn. Waves and Appl.*, Vol. 20, No. 7, 901–912, 2006.
11. Biswas, A., S. Konar, and E. Zerrad, "Soliton-soliton interaction with parabolic law nonlinearity," *J. of Electromagn. Waves and Appl.*, Vol. 20, No. 7, 927–939, 2006.
12. Chen, X., N. Panoiu, and R. Osgood, "Theory of Raman-mediated pulsed amplification in silicon-wire waveguides," *IEEE J. Quantum Electron.*, Vol. 42, No. 2, 160–170, 2006.
13. Soref, R. and B. Bennett, "Electrooptical effects in silicon," *IEEE J. Quantum. Electron.*, Vol. QE-23, No. 1, 123–129, 1987.
14. Kung, F. and H. T. Chuah, "A finite-difference time-domain (FDTD) software for simulation of printed circuit board (PCB) assembly," *Progress In Electromagnetics Research*, PIER 50, 299–335, 2005.
15. Gong, Z. Q. and G. Q. Zhu, "FDTD analysis of an anisotropically coated missile," *Progress In Electromagnetics Research*, PIER 64, 69–80, 2006.
16. Chen, X., D. Liang, and K. Huang, "Microwave imaging 3-D buried objects using parallel genetic algorithm combined with FDTD technique," *J. of Electromagn. Waves and Appl.*, Vol. 20, No. 13, 1761–1774, 2006.